Title
LASER SCANNING MEASUREMENT OF THE DENSITY DISTRIBUTION OF CONFINED 6Li+ IONS

Author
Knight, R.D.

Publication Date
1978-08-01

Submitted to the JOURNAL OF APPLIED PHYSICS

LASER SCANNING MEASUREMENT OF THE DENSITY DISTRIBUTION OF CONFINED $^{6}Li^{+}$ IONS

R. D. Knight and M. H. Prior

August 1978

Prepared for the U. S. Department of Energy
under Contract W-7405-ENG-48

Laser Scanning Measurement of the Density Distribution of Confined $^6Li^+$ Ions.*

R.D. Knight
and
M.H. Prior

University of California, Physics Department
and
Materials and Molecular Research Division,
Lawrence Berkeley Laboratory

Berkeley, California 94720

ABSTRACT

The density distribution of metastable $1s2s\,^3S_1$ Li^+ ions confined in a radio-frequency quadrupole ion trap has been studied using a laser scanning technique. The laser beam, resonant with the 5485Å $1s2s\,^3S_1$ - $1s2p\,^3P_1$ transition, is scanned in a plane normal to the trap z - axis. Intercombination photons, $1s^2\,^1S_0$ - $1s2p\,^3P_1$ at 202Å, are counted and stored as a function of laser beam position. Application of the Abel transform to the data gives the density profile in the plane of the scan. In all cases, the density profiles were consistent with a Gaussian distribution of ions. The radial and axial widths of the distribution were measured as a function of the number of ions and potential well depth and shape. The results are discussed in terms of a model in which the ions are in thermal equilibrium at a temperature of several thousand degrees Kelvin.

INTRODUCTION

During the past twenty years, various types of ion storage devices, including RF-quadrupole ion traps, Penning traps, and electrostatic ion traps, have come to be increasingly versatile and important tools in atomic and molecular physics. Experiments performed in these devices include measurements of hyperfine structures, excited state lifetimes, collisional cross sections, and magnetic moments.[1] In addition, ion traps are now being considered for use as primary frequency standards.

Despite the extensive experience obtained with ion traps, no clear picture has emerged as to the distribution of ions in a trap, average ion energies, or the collisional processes responsible for ion relaxation and eventual loss. This is in large part due to the complexity of the problem, which has hindered all but simplified theoretical models. In addition, experimental results have largely been limited to determinations of the total number of ions and measurements of Doppler widths of spectral lines. Only recently have some results indicated the approximate size of the ion cloud.[2]

In order to understand better the dynamics of ion confinement, in connection with our program of metastable ion lifetime measurements, we have determined the density distribution of metastable 2^3S_1 $^6Li^+$ ions stored in an RF-quadrupole ion trap for various shapes and depths of the effective potential well. These results are relevant to many RF ion trap experiments, particularly where mean energies are needed to estimate reaction rates, while the technique itself can be adapted to studying appropriate ions in other types of traps. In addition, the technique has possible value as a diagnostic tool for studying impurity ions in plasmas.

METHOD

The experimental arrangement is shown in Fig. 1. All timing and data collection are controlled by a PDP-11 computer. The ion trap is of the RF-quadrupole variety and of size $r_o = z_o = 3$ cm. The end electrodes are accurately machined copper hyperboloids, while the ring electrode is a wire mesh which allows good optical access to the trap interior. Li^+ ions are created near the center of the trap by electron bombardment of a Li atomic beam with an axial electron beam passing through a hole in one end cap. The total number of Li^+ ions is monitored by resonant sideband excitation and tuned circuit detection.[1] Typical parameters are $\simeq 10^5$ ions stored with storage lifetimes $\simeq 15$ sec. at a residual background pressure $\simeq 10^{-9}$ Torr. Of these, only some $\simeq 10^3$ are in the metastable 2^3S_1 state.

The energy levels utilized are shown in Fig. 2. The ions studied here are those in the highly metastable 2^3S_1 state. This state is observed to have an effective lifetime $\simeq 5$ sec. at 10^{-9} Torr and is lost primarily by non-radiative quenching collisions (among which we include ion-molecule reactions) with the background gases. The spontaneous radiative lifetime is $\simeq 50$ sec.[3] The metastables are detected by the 202Å intercombination photons from 2^3P_1 to the ground state following the 2^3S_1-2^3P_1 resonant absorption of 5485Å laser photons. The branching ratio of the intercombination decay to the allowed decay back to 2^3S_1 is $\simeq 1:1200$.[4] Using a dye laser producing 50-100 mW power and linewidth $\Delta\lambda \lesssim .05$Å, the entire metastable population can be pumped to the ground state in $\lesssim .3$ sec., with each ion emitting a 202Å photon. We term this process "laser quenching." In this work 96% enriched ^6Li was used; it has much smaller hyperfine structure than ^7Li which makes the laser quenching more efficient for our laser bandwidth. The 202Å photons are detected by windowless electron multipliers. Collection efficiency is increased by grazing incidence light pipes with 200Å thick platinum coatings. Charged particles and metastable neutrals are prevented from reaching the detectors by 800Å thick aluminum foils which are > 50% transmitting at 200Å. The detectors are insensitive to scattered laser light, and the primary background is due to the dark rate (<1/sec) and spontaneous 2^3S_1 decay photons at 210Å.

Data are collected by rapidly scanning the laser beam in a plane normal to the trap z-axis and storing photon counts in a multichannel scaler whose timebase is synchronized with the scan. As discussed below, this produces a signal from which the ion density distribution can be determined. The scanning is accomplished by a small mirror mounted on the movement of a standard relay which is driven by a sinusoidal voltage at its mechanical resonant frequency of ≃50Hz. With the mirror 1.5m from the trap, this easily produces a scan ≃10 cm. wide whose frequency and amplitude are quite stable for the duration of a run (≃1 hour). The portion of the scan which passes through the trap falls on a plate containing narrow slits oriented normal to the scan plane and spaced .10 inch apart with a photodiode mounted behind. The photodiode output as the scan passes across the slits is a series of pulses which can also be stored in the multichannel scaler and used to calibrate the channel number in terms of distance from the trap z-axis. Due to the fact that the laser intersects the ion cloud only for a very small range near the center of its scan, the scan was never observed to be other than linear in time.

The signal obtained is related to the ion density as follows (see Fig. 3). At any instant of time, the signal count rate is given by

$$\frac{dN}{dt} = \varepsilon \int \rho(\vec{r})n(\vec{r})d^3r \qquad (1)$$

where $\rho(\vec{r})$ is the laser power density, $n(\vec{r})$ is the ion density, and ε includes dipole matrix elements, branching ratios, efficiencies, etc. Since the laser power is zero except along the line of the laser beam, parallel to the x-axis, and is constant (the sample being optically very thin), the count rate can be written

$$\frac{dN}{dt}(y,z) = CP\int_{-\infty}^{\infty} n(x,y,z)dx \qquad (2)$$

where y and z now locate the laser beam with respect to the trap center and P is the total laser power. In a precise experiment, the finite width of the laser beam would need to be taken into account, but in our case it is small (<1mm) compared to the ion cloud and would only be a small correction. Now in practice, of course, the laser beam is moving, but its motion (≃.5mm) during one channel width (Δt=20μsec) is small compared to the size of the ion cloud, so we can consider it fixed for each channel. The signal recorded in the i-th channel is then

$$S_i(y_i,z) = \frac{dN}{dt}(y_i,z)N_s\ \Delta t = C'N_sP\int_{-\infty}^{\infty} n(x,y_i,z)dx \qquad (3)$$

where N_s is the total number of scans.

Note two assumptions implicit here: First, we assume the density is constant in time for the length of time the laser is scanning, and second, we assume that the laser depletes metastable ions at a rate slow compared to the mixing time of ions in the cloud. We can estimate the mixing time to be roughly the time for loss of coherence after resonant excitation of the ion motion. This has been observed to be ≃30msec., whereas the metastable depletion time due to laser quenching is several seconds since the laser is outside the trap during most of each scan. The data for each filling of the trap is always collected in <1 sec., which is short compared to the metastable lifetime of ≃5 sec., so the density should remain nearly constant during the collection period. This has been verified by using collection times varying between .1 sec. and 1 sec. following storage periods of .1 sec. to 2 sec. No significant variation in the laser scan profiles has been observed, which indicates that the ion cloud has reached a quasi-equilibrium in $\lesssim$.1 sec. and remains constant in shape thereafter. In order to maintain a particular standard, all work described here used a 1 sec. storage period after ion creation followed by a 1 sec. data collection period. Total time to collect a complete curve was $\simeq$1 hour.

To extract the density distribution from the signal, we utilize the cylindrical symmetry of the trap to write $n(x,y,z) = n(r,z)$. Changing to cylindrical coordinates and writing the signal now as a continuous function, we have

$$S(y,z) = 2C'N_sP \int_y^\infty \frac{n(r,z)r\,dr}{\sqrt{r^2-y^2}} \tag{4}$$

This integral equation for $n(r,z)$ can be solved by utilizing the Abel transforms,[5] which are:

$$g(\xi) = \sqrt{\frac{2}{\pi}} \int_\xi^\infty \frac{f(\eta)}{\sqrt{\eta^2-\xi^2}}\,d\eta \tag{5}$$

$$f(\eta) = -\sqrt{\frac{2}{\pi}} \frac{d}{d\eta} \int_\eta^\infty \frac{\xi g(\xi)}{\sqrt{\xi^2-\eta^2}}\,d\xi$$

If we define $2\,C'N_sPrn(r,z) = \sqrt{\frac{2}{\pi}}\,f(r)$,

and $S(y,z) = g(y)$,

then our solution for the density profile at a particular height z is

$$n(r,z) = \frac{-1}{\pi C' N_s P r} \frac{d}{dr} \int_r^{\infty} \frac{y\, S(y,z)}{\sqrt{y^2 - r^2}}\, dy \tag{6}$$

For theoretical reasons and as observed, $n(r,z)$ is very nearly a Gaussian. A direct integration of the Abel transforms shows that a Gaussian is transformed into a Gaussian, so if we represent our data by

$$S(y,z) = S_o\, e^{-(y/\Delta)^2}$$

where $S_o = S_o(z)$ and $\Delta = \Delta(z)$, than the integral for $n(r,z)$ gives

$$n(r,z) = \frac{S_o}{\sqrt{\pi} C' N_s P \Delta}\, e^{-(r/\Delta)^2} \tag{7}$$

Since the constant C' is not known, we define a relative density normalized to the laser power P and the number of duty cycles completed N_c ($N_c = N_s$/# scans per cycle):

$$n^*(r,z) = \frac{S_o}{N_c P\, \Delta}\, e^{-(r/\Delta)^2} \tag{8}$$

Note that this really measures only the distribution of metastable ions. Since the ion cloud relaxation due to ion-ion and ion-molecule collisions is observed to be fast (<.1 sec.), we have no cause to think that the metastables are distributed any differently than ground state ions.

The data are then analyzed as follows. The collected data in the multichannel scaler for a given z are first corrected for a small background and then least squares fitted to a Gaussian, yielding values for S_o and Δ. In all cases, the reduced χ^2 indicates that the choice of a Gaussian is indeed appropriate. Using the fitted values along with measured values for P and N_c gives the relative density n*(r,z) as a function of the radius for a slice of the ion cloud at a particular z. Having been normalized, n* is independent of the laser power and the number of duty cycles required to collect the curve. A typical curve is shown in Fig. 4, along with the fitted Gaussian. The apparent structure near channel number 85 is a shadow caused by a section of the ring electrode blocking the laser beam. The points in the shadow have been excluded from the least squares fitting routine.

RESULTS

As stated above, all of our data could be fitted well to a Gaussian and we can thus represent the ion density by $n(r,z) = n_o \exp[-(r/\Delta)^2]$ where $n_o = n_o(z)$ and $\Delta = \Delta(z)$. For a spherical potential well, the "ion radius" Δ and the well depth D determine the average ion energy, so we have been concerned with measuring Δ for various trap parameters. Since we have found the number of ions created to fluctuate occasionally as much as 30% from cycle to cycle, it was of importance to establish first how the ion radius varies with the number of ions stored. Our results at z = 0 with a spherical potential well are shown in Fig. 5. With the possible exception of very small numbers of ions, the radius is seen to be independent of the ion number. All subsequent data were then taken with a sufficient number of ions to eliminate any major error resulting from fluctuations.

Fig. 6 shows the radius at z=0 as a function of the depth of a spherical potential well. This figure also shows a determination of the radius based upon the measured linewidth of the 2^3S_1-2^3P_1 resonance and a simple model of the line shape which assumes the ions have a Gaussian distribution. This model calculates the optical pumping of the various hyperfine levels, assuming no relaxation of the metastable state (a reasonable assumption for ions stored in an ultra high vacuum during the 1 sec. long laser pulse). The laser quenching is strong only when the laser overlaps the Doppler profiles of all the transitions. Note that linewidth measurements alone give only an average energy and cannot yield an ion radius unless some distribution is assumed. The agreement of the radius as determined by the two methods is satisfactory except for possibly the case D=18eV. We observed, however, that data taken at D=18eV on other days generally gave somewhat larger values for Δ which were consistent with the linewidth value. Not being able to verify that all other conditions were identical, such data were not shown in the figure.

In general, the ion trap need not have a spherical potential well but can have a cylindrically symmetric effective potential given by

$$U = \frac{r^2}{r_o^2} D_r + \frac{z^2}{z_o^2} D_z$$

The ion cloud might then be expected to be either compressed or expanded in the radial direction for D_r, respectively, larger or smaller than D_z. If, in addition, the cloud remains a Gaussian of the form

$$n(r,z) = n_o' \exp[-(r/\Delta_r)^2 - (z/\Delta_z)^2] \qquad (9)$$

where n_o' is now constant, then clearly the radius Δ_r is independent of the height z. This would not be the case, for, say, a cloud of constant density and sharp edges. In Fig. 7 are shown the results for Δ_r as a function of the height of the laser scan above the trap center for three differently shaped potential wells, and in Fig. 8 are shown the radial density profiles for one of these wells. The cloud is indeed compressed when D_r is increased while D_z decreases, and Δ_r is seen to have at most slight dependence on z. An analysis of the coefficients S_o/N_cP from Eq. (8), while of limited accuracy, is consistent with a Gaussian distribution along the z-axis in which Δ_z expands concurrently with the contraction of Δ_r when D_r is increased and D_z decreased.

A more careful check of whether the ion cloud is Gaussian along the z-axis was made by measuring the count rate for a stationary laser beam passing through y=0 at various heights z for a spherical potential well. In this case, because of the cylindrical symmetry about the y-axis, the earlier analysis applies equally well to the axial direction and a Gaussian signal yields a Gaussian density profile. In addition, we have shifted the ion cloud away from the trap center by applying a DC voltage ΔV to the lower endcap electrode, while also adjusting the DC voltage on the ring to maintain a well of constant depth. The results are shown in Fig. 9 along with fitted Gaussian curves. The assumption of a Gaussian distribution in the axial direction is seen to be satisfactory and the ion radii Δ_z, which are the same in all three cases, are consistent with measurements of Δ_r made under similar conditions. It is also seen that we have demonstrated the possibility of manipulating the ion cloud over distances comparable to the cloud size, a fact which would be difficult to verify without using the laser to "take a picture" of the ion cloud. A simple model of a uniform electric field being superimposed upon the effective trap field would predict a shift of .5 cm for the parameters used. That the actual shift is somewhat less is likely due to the fact that the DC electric field between the hyperbolic end electrodes is only moderately well approximately by a uniform field in the region occupied by the ions.

DISCUSSION

In the absence of ion-molecule collisions and RF-heating effects, cold ions will reach a steady-state distribution where the space-charge forces and trapping forces just balance.[1] In this limit, the ions fill the potential well at constant density up to a well-defined ion cloud radius determined by the total number of ions, rather like water filling a bowl. This has been observed for charged metallic dust particles in an RF-quadrupole trap since collision processes with the background molecules are insignificant.[6] However, for atomic or molecular ions, these processes provide considerable heating and the cold ion model is not justified. A more reasonable model has been constructed which considers ions at a finite temperature colliding with background molecules but ignores RF-heating.[7] In this case one finds that the ion density distribution is approximately Gaussian and that the equilibrium temperature approaches that of the background gas. However, measurements of the ion temperature in RF-quadrupole traps by bolometric[8] and linewidth[9] techniques generally give $T \simeq 10^4\ {}^oK$ for well depths $D \simeq 10eV$, consistent with our results. This indicates that RF-heating is the dominant mechanism of energy input, an interpretation supported by the fact that ions in a Penning trap, with static fields only, are capable of being cooled to the background gas temperature.[10]

If we hypothesize that the background molecules together with the RF field act as an effective heat reservoir at temperature T, then the ions in equilibrium will obey a canonical distribution such that the probability of finding an ion with velocity in the range d^3v at $\vec{v}$ and position in the range d^3r at $\vec{r}$ is

$$P(\vec{r},\vec{v})d^3rd^3v \propto e^{-E(\vec{r},\vec{v})/kT}\, d^3rd^3v \qquad (10)$$

For ions in a cylindrically symmetry potential well extending to infinity,

$$E(\vec{r},\vec{v}) = \frac{1}{2} mv^2 + \frac{r^2}{r_o^2} eD_r + \frac{z^2}{z_o^2} eD_z \qquad (11)$$

where D_r and D_z are the well depths for a trap of dimensions r_o and z_o. The distribution function $f(\vec{r},\vec{v})$, normalized to

$$\int d^3r d^3v \; f(\vec{r},\vec{v}) = N$$

where N is the total number of ions, is then

$$f(\vec{r},\vec{v}) = \frac{N}{r_o^2 z_o} \frac{(8e^3m^3D_r^2D_z)^{\frac{1}{2}}}{(2\pi kT)^3} \exp\left(- \frac{mv^2}{2kT} - \frac{r^2eD_r}{r_o^2kT} - \frac{z^2eD_z}{z_o^2\, kT}\right) \qquad (12)$$

Integrating over d^3r gives the usual Maxwellian distribution of velocities normally obtained by considering the potential energy to be constant. To obtain the density distribution one integrates over d^3v and finds

$$n(\vec{r}) = \frac{N}{r_o^2 z_o} \left[\frac{e^3D_r^2\, D_z}{(\pi kT)^3}\right]^{1/2} \exp[(-r/\Delta_r)^2 - (z/\Delta_z)^2] \qquad (13)$$

where

$$\Delta_r = r_o\sqrt{kT/eD_r}$$

$$\Delta_z = z_o\sqrt{kT/eD_z}$$

This is identical to Eq. (9). In a practical situation, however, one can only integrate over the trap volume rather than to infinity. But as long as $\Delta_r << r_o$

and $\Delta_z \ll z_o$ the error is small and the distribution should be very close to Gaussian.

Without a detailed model there is, of course, no rigorous justification for the hypothesis that the ions are in contact with an effective heat reservoir determined by the molecules and RF field. The agreement of our measurements with the distribution predicted by this model does, however, provide strong evidence that this hypothesis is correct. In particular: (1) We observe that the ion cloud is in quasi-equlibrium over times long compared to relaxation times; (2) In all cases our data is consistent, to within statistical errors, with a Gaussian density distribution; (3) The ion cloud radius has, at most, only slight dependence on the total number of ions, indicating that ion-ion collisions do not play a major role in the dynamics of the ion cloud. The Gaussian distribution with its implied Maxwellian velocity distribution also confirms the idea, introduced by Dehmelt[1], that the ions can, in fact, be described by a temperature - a concept which would have little meaning if the distribution were substantially different. The equilibrium temperature for a given well depth will be determined by balancing the RF - heating with energy loss mechanisms such as collisions and ion evaporation. It is then likely that the temperature varies with the well depth, and this would explain why Δ does not seem to fall off as rapidly as $D^{-\frac{1}{2}}$ in Fig. 6.

A Gaussian density distribution greatly simplifies many calculations, such as mean velocities or Doppler-widths, and allows results to be stated in terms of the well depth (a known parameter) and Δ. For example, in a spherical well the average potential energy is

$$\langle eU \rangle = \frac{\int n(\vec{r})\, eU(\vec{r})\, d^3r}{\int n(\vec{r})\, d^3r} = \frac{3}{2}\frac{\Delta^2}{r_o^2}\, eD$$

From the Virial Theorem for a harmonic oscillator, the mean total energy is just twice this, so

$$E = 3kT = 3 \frac{\Delta^2}{r_o^2} eD$$

The values of Δ observed in this work imply temperatures $T \simeq 5000^oK$, consistent with other measurements mentioned previously.

CONCLUSION

We have reported results of the first detailed determination of the distribution of ions in an RF-quadrupole ion trap. The Gaussian-shaped profiles which are independent of the total ion number support the hypothesis that RF-heating in collisions with background gas molecules is the major factor determining the ion cloud dynamics. The laser scanning technique utilized in this work could be profitably applied to other types of ion traps.

This work was supported by the Division of Chemical Sciences, Office of Basic Energy Sciences, U. S. Department of Energy.

REFERENCES

*Work supported by the Chemical Sciences Division, Office of Basic Energy Sciences, U.S. Department of Energy.

[1]The basic theory and techniques of ion storage as well as many applications are reviewed in H.G. Dehmelt, Adv. At. Mol. Phys. 3, 53 (1967); 5, 109 (1969). See also F.L. Walls and G.H. Dunn, Phys. Today 27, 30 (Aug. 1974).

[2]D.J. Wineland, R.E. Drullinger, and F.L. Walls, Phys. Rev. Lett. 40, 1639 (1978); W. Neuhauser, M. Hohenstatt, P. Toschek, and H. Dehmelt, Phys. Rev. Lett. 41, 233 (1978).

[3]G.W.F. Drake, Phys. Rev. A3, 908 (1971).

[4]G.W.F. Drake and A. Dalgarno, Astrophys. J. 157, 459 (1969).

[5]I.N. Sneddon, The Use of Integral Transforms, pp. 318-19 (McGraw-Hill, New York, 1972).

[6]R.F. Wuerker, H. Shelton, and R.V. Langmuir, J. Appl. Phys. 30, 342 (1959).

[7]J. André, J. Physique 37 719 (1976).

[8]D.A. Church and H.G. Dehmelt, J. Appl. Phys. 40, 3421 (1969).

[9]R. Iffländer and G. Werth, Metrologia 13, 167 (1977).

[10]H.G. Dehmelt and F.L. Walls, Phys. Rev. Lett. 21, 127 (1968).

FIGURE CAPTIONS

Fig. 1 Experimental arrangement for measuring ion density profiles with scanned laser beam. Only one of two detectors is shown.

Fig. 2 Li^+ energy levels pertinent to this work.

Fig. 3 Scanning geometry for an ellipsoidal ion cloud. The laser beam is scanned in a plane parallel to the x-y plane at a set height z to determine n(r,z).

Fig. 4 Representative set of data. The structure near channel 85 is a shadow of a portion of the trap structure. The curve is a least squares fitted Gaussian.

Fig. 5 Ion cloud radius versus number of ions stored in a spherical potential well.

Fig. 6 Ion cloud radius for different spherical potential well depths. The points without error bars were independently determined from the linewidth of the intercombination signal measured by varying the laser wavelength.

Fig. 7 Ion cloud radius at different heights above the trap center for three potential well shapes: Dots, D_r = 24eV, D_z = 6eV; squares, $D_r = D_z$ = 18eV; triangles, D_r = 9eV, D_z = 36eV.

Fig. 8 Radial density profiles at three scan heights for the case D_r = 9eV, D_z = 36eV. Data is shown only for the z = 0.25cm scan excluding the shadow region. The curves are the fitted Gaussians and have the same width.

Fig. 9 Axial density profiles for a spherical potential well, $D_r = D_z$ = 18eV, with different values of ΔV applied to the lower endcap: Triangles, ΔV = 12V; dots, ΔV = 0; and squares, ΔV = -12V.

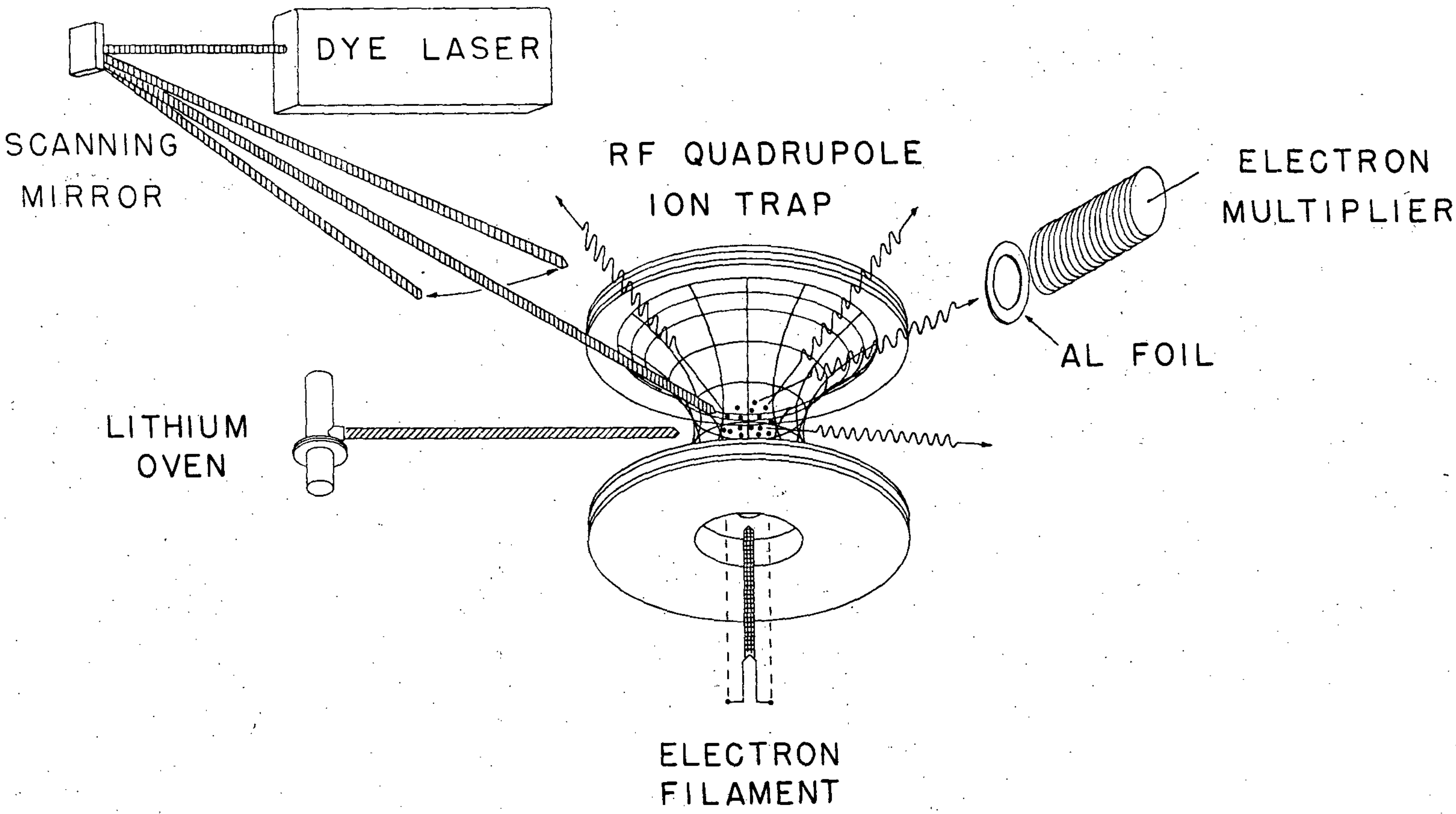

XBL 788-10366

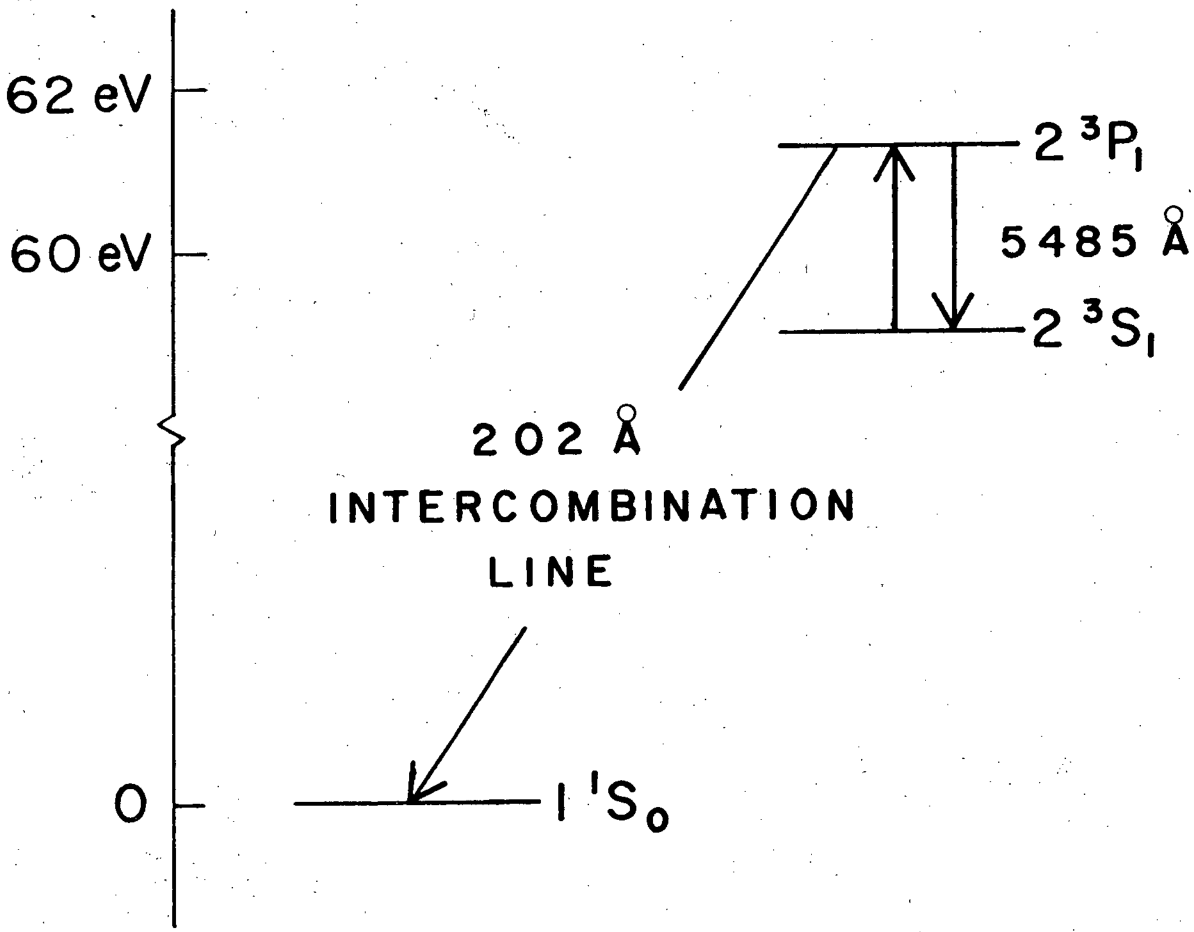

XBL 788-10373

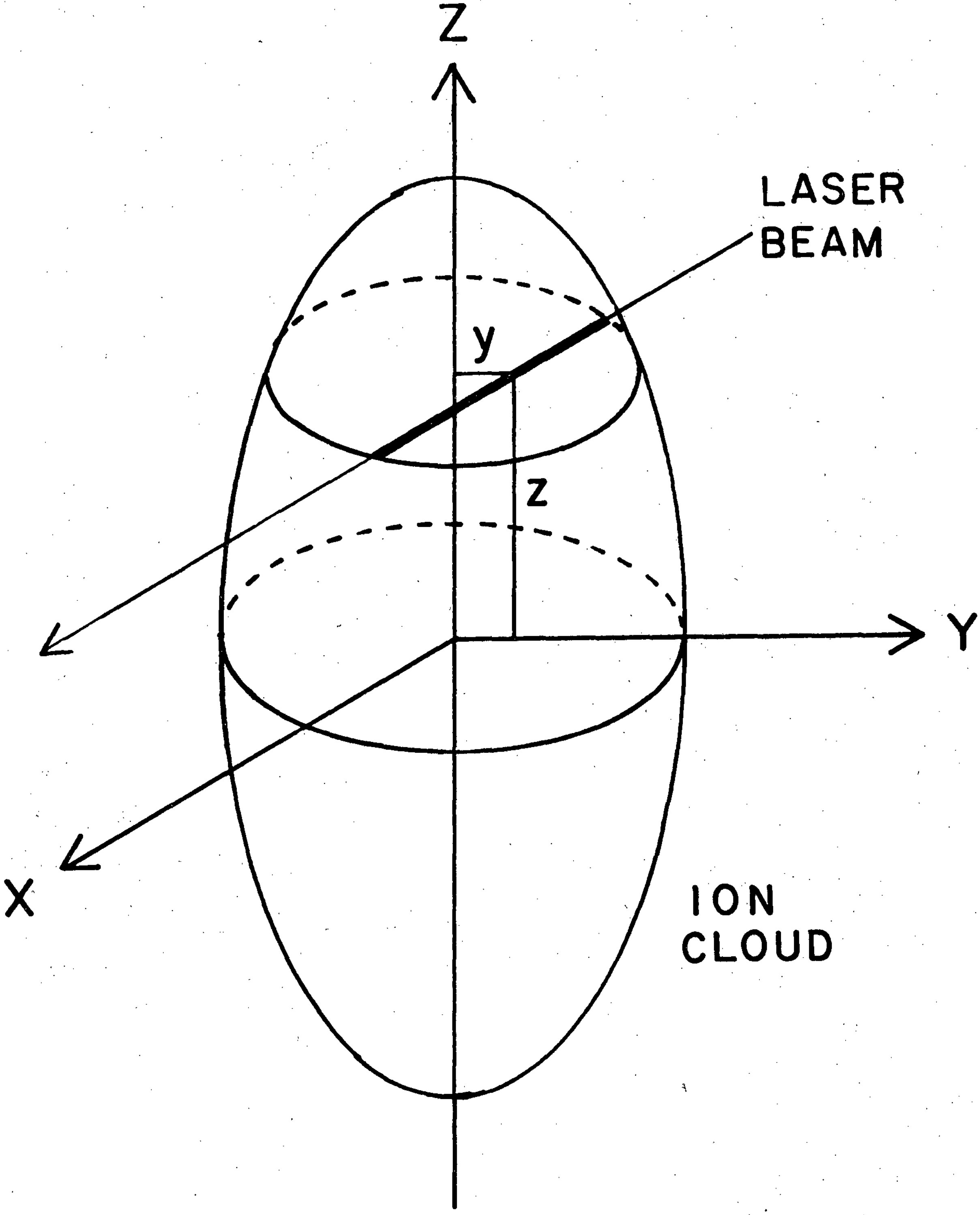

XBL 788-10374

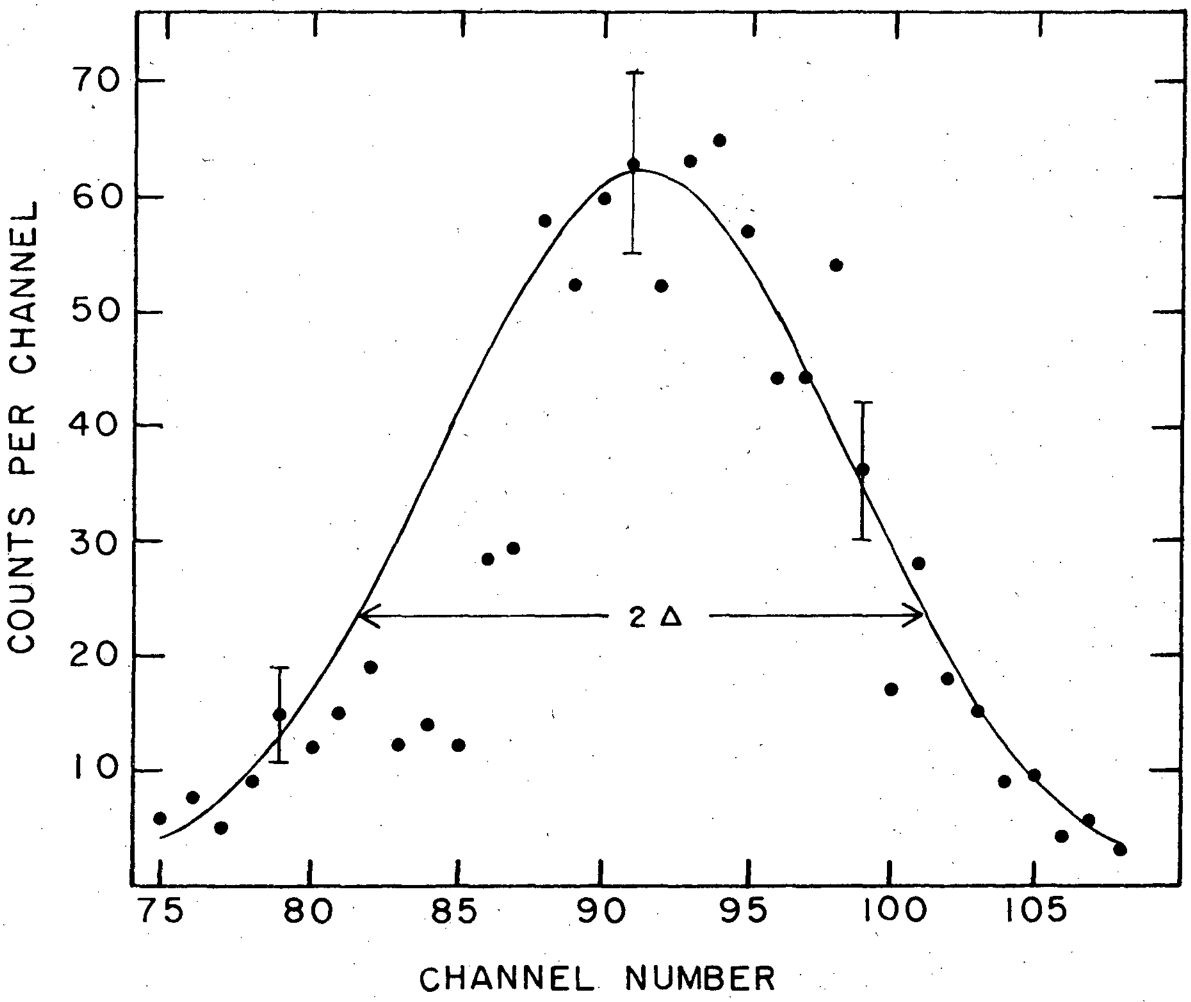

XBL 788-10368

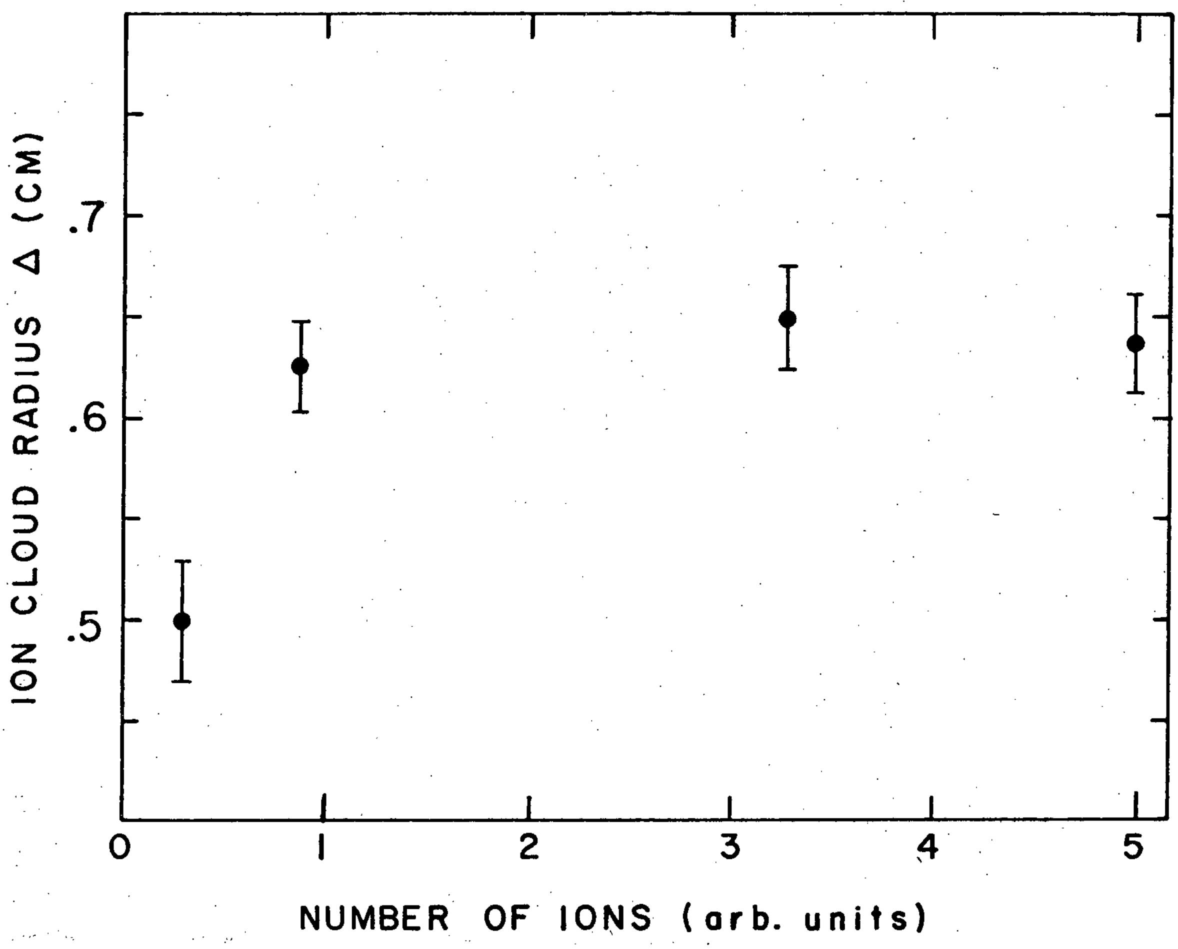

XBL 788-10370

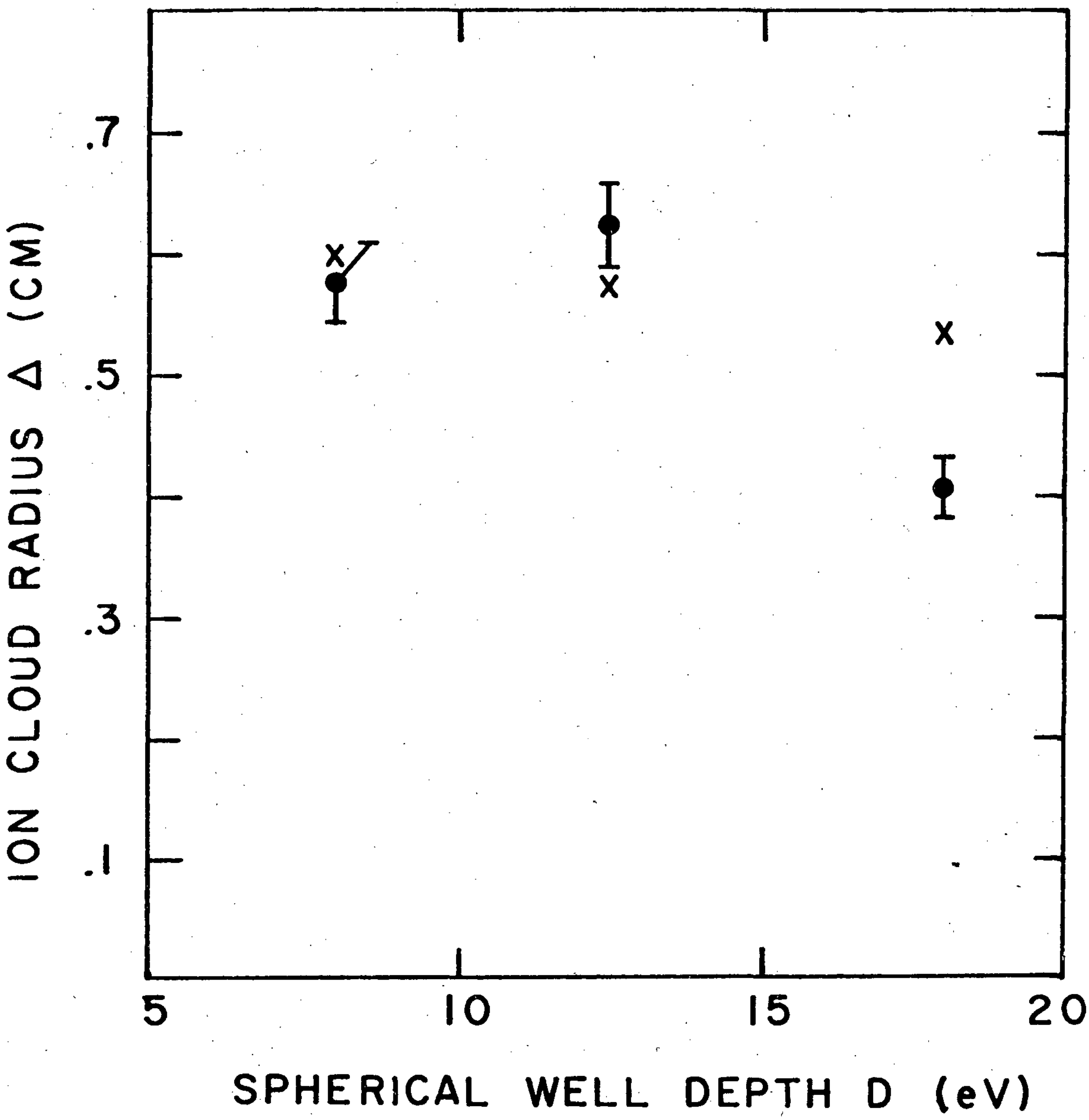

XBL 788-10371

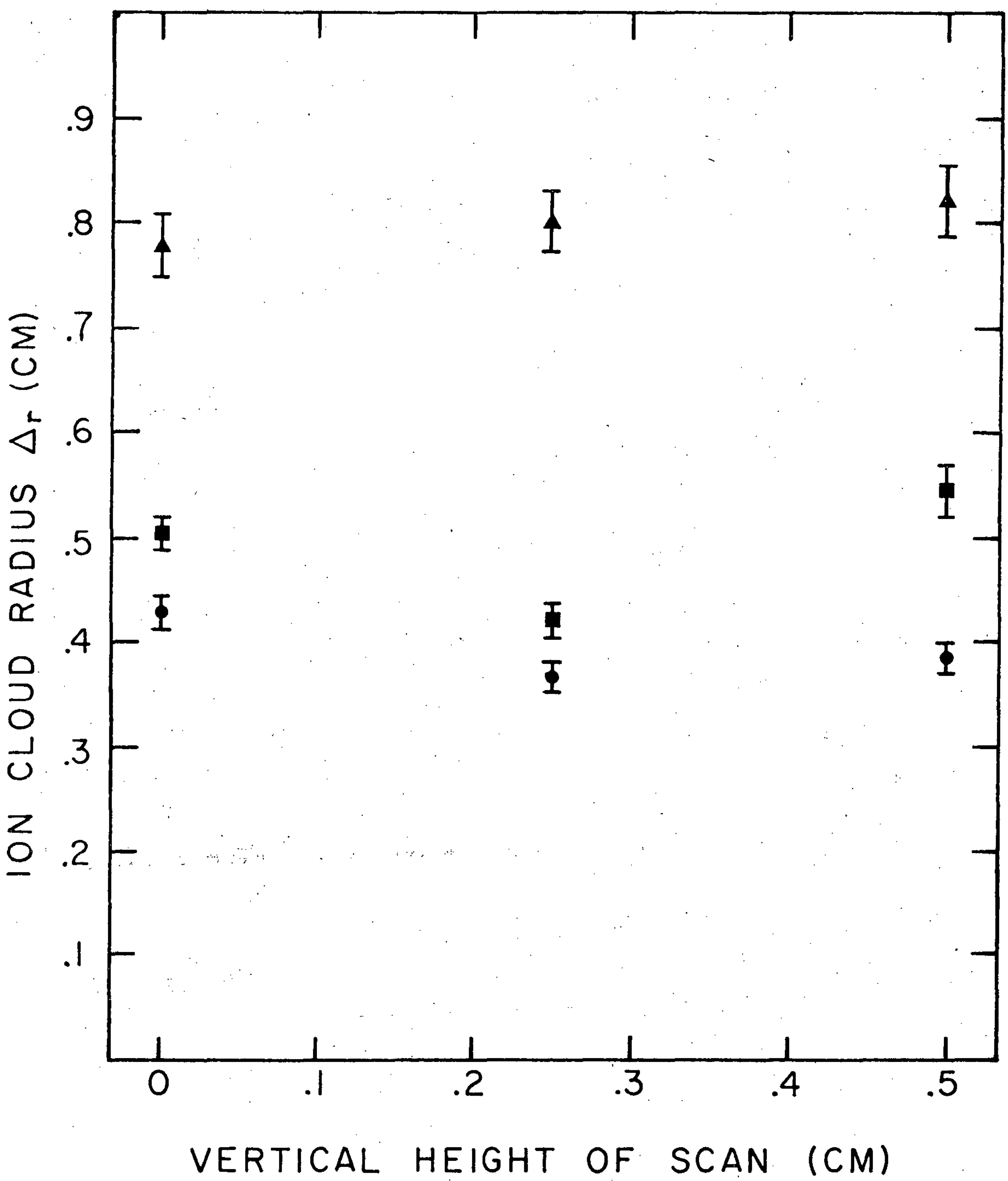

XBL 788-10367

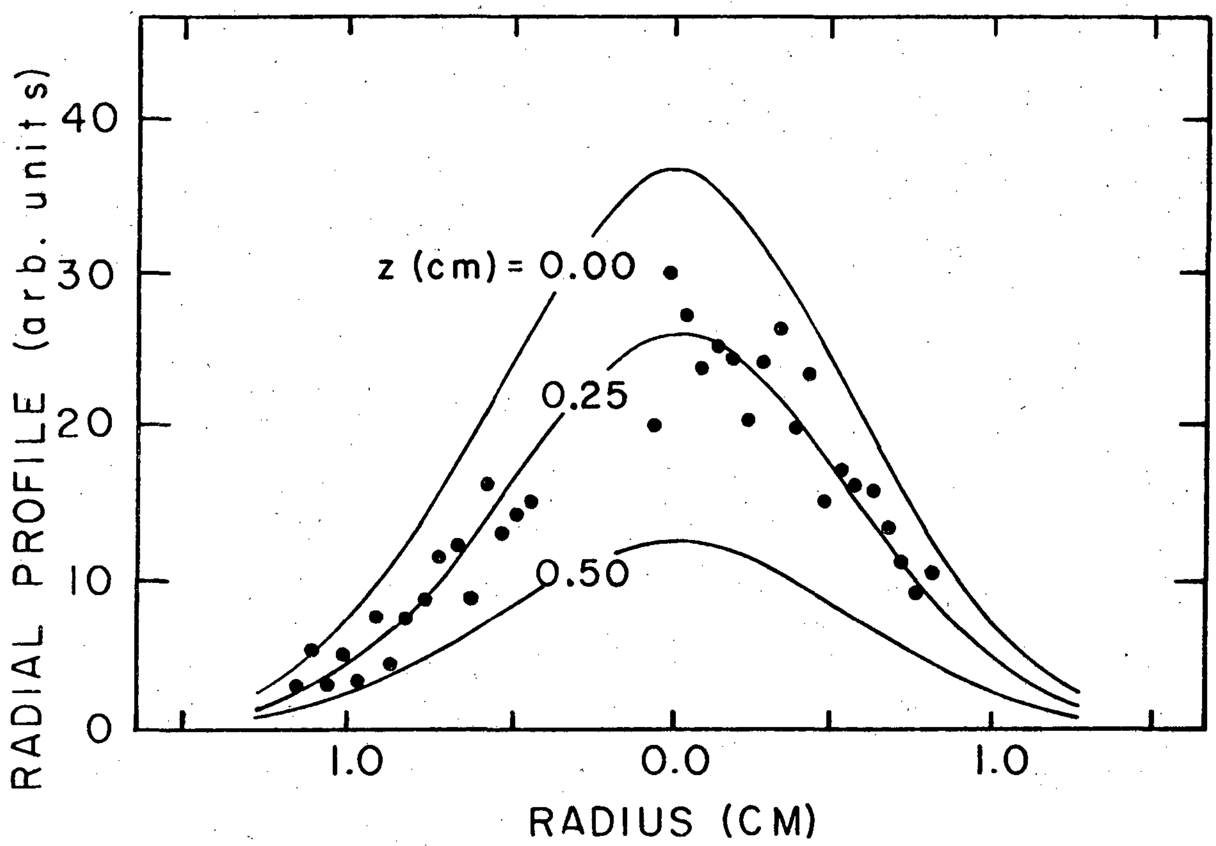

XBL 788-10372

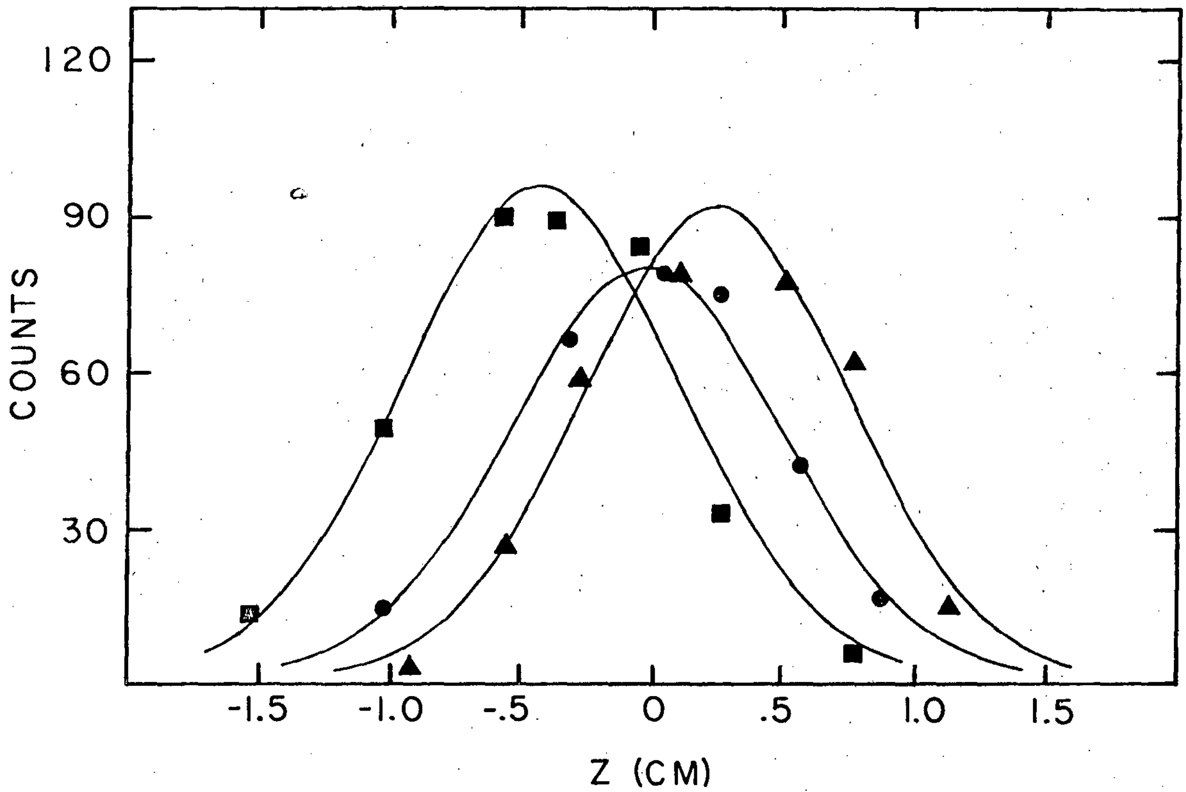

XBL 788-10369

TECHNICAL INFORMATION DEPARTMENT
LAWRENCE BERKELEY LABORATORY
UNIVERSITY OF CALIFORNIA
BERKELEY, CALIFORNIA 94720